Ordering spatiotemporal chaos in complex thermosensitive neuron networks

Yubing Gong,[1] Bo Xu,[1] Qiang Xu,[1] Chuanlu Yang,[1] Tingqi Ren,[1] Zhonghuai Hou,[2,*] and Houwen Xin[2]
[1]*Department of Physics, Yantai Normal University, Yantai, Shandong 264025, People's Republic of China*
[2]*Department of Chemical Physics, University of Science and Technology of China, Hefei, Anhui 230026, People's Republic of China*
(Received 21 November 2005; revised manuscript received 14 February 2006; published 28 April 2006)

We have studied the effect of random long-range connections in chaotic thermosensitive neuron networks with each neuron being capable of exhibiting diverse bursting behaviors, and found stochastic synchronization and optimal spatiotemporal patterns. For a given coupling strength, the chaotic burst-firings of the neurons become more and more synchronized as the number of random connections (or randomness) is increased and, rather, the most pronounced spatiotemporal pattern appears for an optimal randomness. As the coupling strength is increased, the optimal randomness shifts towards a smaller strength. This result shows that random long-range connections can tame the chaos in the neural networks and make the neurons more effectively reach synchronization. Since the model studied can be used to account for hypothalamic neurons of dogfish, catfish, etc., this result may reflect the significant role of random connections in transferring biological information.

DOI: 10.1103/PhysRevE.73.046137 PACS number(s): 89.75.Hc, 05.45.Xt

I. INTRODUCTION

Dynamical processes in complex networks have attracted growing attention in recent years [1–3]. Studies have been focusing on the small-world network (SWN) [4] and scale-free network (SFN) [5] due to their importance in explicitly mimicking a highly complex structure of many realistic social [6], biological [7,8], or electronic communication [9–11] networks. So far, studies on complex networks can be divided into two main categories: In the dominant category, investigations are concerned with the topological properties of complex networks and various mechanisms to determine the topology; in the other more important category, research is engaged in understanding how the network topology influences the system's dynamic features. Studies show that any spreading rate can lead to the whole infection of disease on SFN [12,13]; stochastic resonance [14] and synchronization [15,16] can be considerably improved on SWN, and SWN can greatly enhance the probability of spiral wave formation in excitable media [17], ordering chaos [18], and oscillator death [19]. All these studies show that random shortcuts play a crucial role in the system's dynamics.

In biology, neural networks have always been an important subject of research. It is well known that a single neuron in the vertebrate cortex connects to more than 10 000 postsynaptic neurons via synapses forming complex networks [20]. Therefore, it is necessary to employ networks to account for the dynamics of neural systems, and randomly adding a number of long-range shortcuts among neurons representing random connections is reasonable and feasible. One of the important dynamical phenomena, regarding the effects of random connectivity of networks, is the enhancement of synchronization of spikes since the synchronization of coupled neurons may elucidate how the coherent spontaneously synchronized oscillations, which have been observed in the brain cortex, are established in many neural systems [21–23].

Braun *et al.* [24] proposed a modified Hodgkin-Huxley (MHH) model of thermally sensitive neurons that mimics all spike train patterns observed in electroreceptors from dogfish [25], catfish, and facial cold receptors [26]. All these neurons can be characterized by spontaneous, noisy oscillations that are reflected in spike or burst trains. A lot of studies have been dedicated to the dynamics of the MHH model due to its rich nonlinear behaviors. The single MHH neuron model exhibits various bursting behaviors as temperature T is varied [24], and burst-enhanced synchronization and various synchronization regimes with the increase of coupling strength were observed in the coupled neurons [27]. The bifurcation diagram [28] and phase-space structure [29] of the MHH neuron have been discussed in detail. It shows that as the temperature is decreased, the system undergoes a series of period-adding bifurcations, corresponding to transitions between various bursting states, and after a critical value of T, the system undergoes a homoclinic bifurcation, followed by an inverse period-doubling cascade. Therefore, an intriguing and significant question arises: How does the complex network topology affect the spatiotemporal chaotic dynamics of the coupled MHH neuron system?

In this paper, we have investigated the dynamics of chaotic MHH neurons on complex networks. The complex network is constructed by randomly adding long-range links (shortcuts) to an originally nearest-coupled one-dimensional neuron chain. We mainly focus on how the topological randomness p, defined as the fraction of random shortcuts, would affect the system's spatiotemporal evolution. The parameters chosen can only sustain spatiotemporal chaos in the original regular neuron network. We find that chaotic burst-firings become appreciably and more and more synchronized in space and periodic in time with the addition and increase of random shortcuts, and at an optimal value of p a most ordered spatiotemporal behavior appears, which indicates all neurons undergo periodic synchronized oscillations. Further increasing random shortcuts, however, would destroy the periodicity in time though it can enhance the synchronization in

*Author to whom correspondence should be addressed. Electronic mail: hzhlj@istc.edu.cn

space. We have introduced an order parameter to characterize the spatiotemporal regularity of the neurons' motion, which shows a clear maximum with the variation of p. These phenomena imply that topological randomness can tame the spatiotemporal chaos in the MHH neurons. We have also studied the effects of the coupling strength and found that the value of the optimal randomness p decreases when the coupling strength increases.

II. MODEL AND EQUATIONS

The model here is the coupled MHH neurons on a complex network. The network is constructed as follows: It starts with a one-dimensional regular chain which comprises $N=60$ identical chaotic MHH neurons. Each neuron is connected to its two nearest neighbors. Links are then randomly added between non-nearest vertices. In the limit case where all neurons are coupled to each other, the network contains at most $N(N-1)/2$ edges. Using M to denote the number of added shortcuts, then the fraction of the shortcuts, which is the ratio of random shortcuts to all possible number of edges among the neurons, reads $p=M/[N(N-1)/2]$, which can be used to characterize the randomness of the network. Note that for a given p there are a lot of network realizations.

In the presence of the coupling between neurons, the membrane potential of each neuron is given by

$$C_M\frac{dV_i}{dt} = -I_{il} - I_{iNa} - I_{iK} - I_{isd} - I_{isr} + \xi_i + \sum_j g_{ij}(V_j - V_i), \tag{1}$$

where C_M is the membrane capacitance, ξ_i denotes the noise in each neuron, and $\Sigma_j g_{ij}(V_j-V_i)$ represents the coupling between two neurons. The currents on the right-hand side fall into three groups. The first two, I_{iNa} and I_{iK}, are the fast sodium and potassium currents that generate the action potentials,

$$I_{iNa} = \rho g_{Na} a_{Na}(V_i - V_{Na}), \tag{2}$$

$$I_{iK} = \rho g_K a_K (V_i - V_K), \tag{3}$$

where the g's are the conductances and the a's contain the switching characteristics of the channels. In the steady state

$$a_{Na,\infty} = a_{K,\infty} = \frac{1}{1+\exp[-0.25(V_i + 25\text{mV})]}. \tag{4}$$

The sodium and potassium currents relax exponentially

$$\frac{da_{Na}}{dt} = \frac{\phi}{\tau_{Na}}(a_{Na,\infty} - a_{Na}), \tag{5}$$

$$\frac{da_K}{dt} = \frac{\phi}{\tau_K}(a_{K,\infty} - a_K). \tag{6}$$

The dimensionless factors ρ and ϕ contain the temperature dependence

$$\rho = 1.3^{(T-T_0)/10}, \tag{7}$$

TABLE I. Values of parameters used in the model.

Membrane capacitance $C_M=1$ (μF/cm^2)	
Conductances (m S/cm^2)	
$g_{Na}=1.5$	$g_K=2.0$
$g_{sd}=0.25$	$g_{sa}=0.4$
$g_l=0.1$	
Time constants (ms)	
$\tau_{Na}=0.05$	$\tau_k=2.0$
$\tau_{sd}=10$	$\tau_{sa}=20$
Reversal potentials (mV)	
$V_{Na}=V_{sd}=50$	
$V_K=V_{sa}=-90$	
$V_l=-60$	

$$\phi = 3.0^{(T-T_0)/10}, \tag{8}$$

where the reference temperature $T_0=25$ °C. The next two currents in Eq. (1) describe the slow currents which are given by

$$I_{isd} = \rho g_{sd} a_{sd}(V_i - V_{sd}), \tag{9}$$

$$I_{isa} = \rho g_{sa} a_{sa}(V_i - V_{sa}), \tag{10}$$

where the indices *sd* and *sa* stand for "slow depolarization" and "slow after hyperpolarization." They are resumed to relax according to

$$\frac{da_{sd}}{dt} = \frac{\phi}{\tau_{sd}}(a_{sd,\infty} - a_{sd}), \tag{11}$$

$$\frac{da_{sa}}{dt} = \frac{\phi}{\tau_{sa}}(-\eta I_{isd} - k a_{sa}), \tag{12}$$

where $\eta=0.012$ μA, $k=0.17$, and

$$a_{sd,\infty} = \frac{1}{1+\exp[-0.09(V_i + 40\text{ mV})]}. \tag{13}$$

The temperature dependence is controlled by the same factors ρ and ϕ as above. Finally, the leak current I_{il} is given as

$$I_{il} = g_l(V_i - V_l). \tag{14}$$

The values of all the other parameters that appear in the above equations are listed in Table I.

In the coupling term $\Sigma_j g_{ij}(V_j-V_i)$, V_i and V_j are the membrane potentials of neurons i and j, respectively; $1 \leqslant (i,j) \leqslant N$, here $N=60$ is the number of neurons, and the summation takes over all neurons; g_{ij} is a coupling constant between the two neurons i and j, which is determined by the coupling pattern of the system and is identical for any two neurons, i.e., $g_{ij}=g$. If neurons i and j are connected, they have a constant coupling strength g; otherwise the coupling strength is $g=0$.

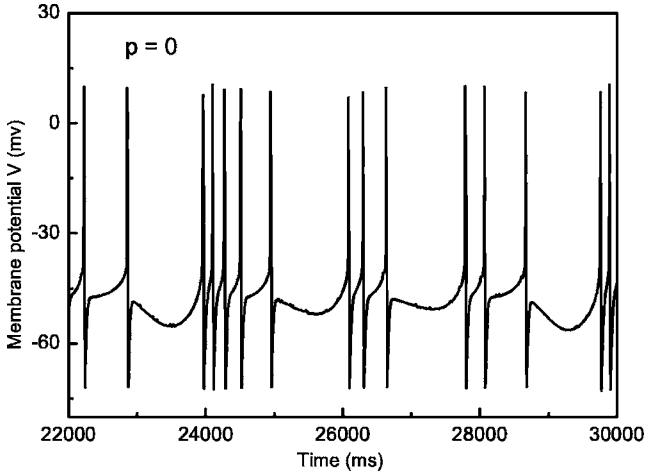

FIG. 1. Chaotic time series of a membrane potential V of a single neuron at $p=0$, i.e., on the regular network.

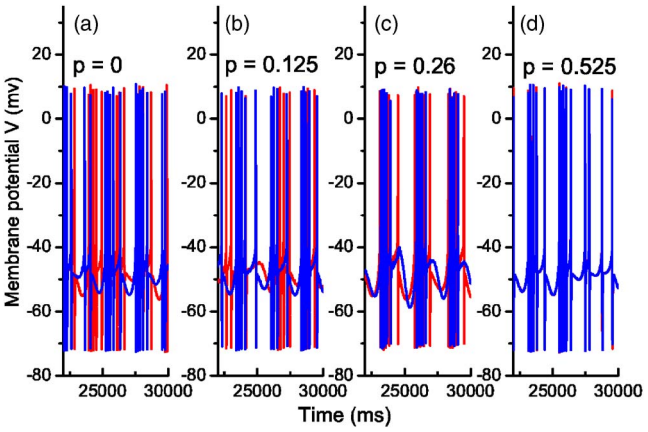

FIG. 2. (Color online) Time series of the membrane potentials of two neurons with various p. The most ordered spatiotemporal behavior appears at $p=0.26$.

The MHH neuron in system (1) is temperature dependent and exhibits distinct dynamical behaviors with various temperatures. It behaves like regular spikes ($T<7.31$ °C), chaotic bursts (7.31 °C$\leqslant T\leqslant$10 °C), and regular bursts ($T>10$ °C) [28]. Here, in order to address the effect of the network topology on the ordering chaos, we fix temperature $T=8.2$ °C, such that the system is located in a chaotic region and hence each neuron shows chaotic bursts. Noises $\xi_{i=1,\ldots,60}$ are Gaussian white ones with $\langle\xi_i\rangle=0$, $\langle\xi_i(t)\xi_j(t)\rangle_{i\neq j}=0$, and $\langle\xi_i(t)\xi_i(t')\rangle=D\delta(t-t')$, where D represents the noise intensity.

Numerical integrations of Eq. (1) are performed by using the explicit Euler method with time step 0.01 ms. Periodic boundary conditions are employed and the parameter values for all the neurons are identical except for distinct initial values of potential V_{i0} and the noise terms ξ_i for each neuron.

III. RESULTS AND DISCUSSION

The bifurcation of a single neuron, i.e., the system (1) in the absence of the coupling term $\Sigma_j g_{ij}(V_j-V_i)$, has been described in detail in Ref. [28] and hence is not repeated here. We study the system (1) by fixing the coupling strength $g=0.001, 0.002, 0.003, 0.004$ and noise level $D=0.0005, 0.005, 0.05, 0.1$, and let the fraction of random shortcuts p be variable. All other parameters are the same as given above.

We first fix $D=0.05$ and choose $g=0.002$. For each p, the average over 50 calculations (i.e., realizations of networks) is performed, and in each calculation the initial values of 60 neurons' membrane potentials are newly chosen randomly. At the beginning, we let $p=0$, i.e., all neurons are located on the regular ring and there is not any random shortcut added to the chain. In this case, each neuron behaves like chaotic bursts (Fig. 1), and all neurons do not synchronize their bursts either. To check the evolution of the temporal periodicity and spatial synchronization of different neurons with changing p, we give the comparison of the time series of membrane potentials of two neurons in Fig. 2 and the spatiotemporal evolution of all 60 neurons in Fig. 3. In Fig. 3 the narrow structures in the brighter regions correspond to the firing patterns of individual spikes inside a burst. The left panels in Figs. 2 and 3 correspond to the case $p=0$, i.e., in the regular network, they show that the bursts are chaotic without random shortcuts. As p is increased, the bursts become appreciably ordered [Figs. 2(b) and 3 for $p=0.125$]. As p is increased to $p=0.26$, the bursts reach the most ordered spatiotemporal state where they become the most temporally periodic and considerably spatially synchronized [Figs. 2(c) and 3 for $p=0.26$]. However, as p is further increased, the temporal periodicity becomes worse, while the spatial synchronization evolves better [Figs. 2(d) and 3 for $p=0.525$].

These spatiotemporal evolutions of membrane potentials of 60 coupled neurons on the complex network with p shows

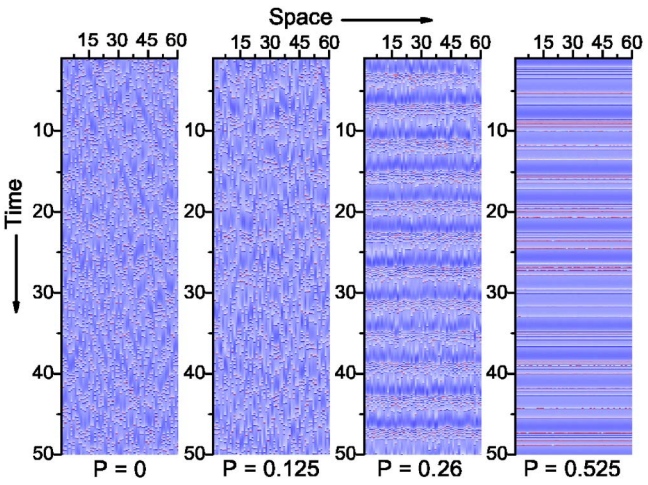

FIG. 3. (Color online) Spatiotemporal evolution of membrane potentials of 60 coupled neurons on the complex network for four typical values $p=0$, 0.125, 0.26, 0.525, with $D=0.05$ and $g=0.002$. The most ordered spatiotemporal behavior of bursting appears at $p=0.26$. In each panel, the abscissa represents the neurons and the ordinate represents the time changing from top to bottom. The bright regions show the firing of neurons, while the dark regions show the quiescence of them.

that random shortcuts benefit the synchronization of chaotic bursts and, more important, there exists an optimal topological randomness such that the system has the maximal order and the spatiotemporal chaos is tamed.

To quantitatively characterize this behavior, we introduce the characteristic correlation time $\tau(p)$ and standard deviation σ to measure the temporal regularity and spatial synchronization of the spatiotemporal patterns, respectively. The characteristic correlation time for measuring the regularity is based on the normalized autocorrelation function $c_i(\tau_d)$, defined as

$$c_i(\tau_d) = \langle \bar{V}_i(t)\bar{V}_i(t+\tau_d)\rangle / \langle \bar{V}_i^2 \rangle, \tag{15}$$

where $V_i(t)$ is the membrane potential of the ith neuron at time t, τ_d is the time delay, $\bar{V}_i(t) = V_i(t) - \langle V_i(t)\rangle$, and the averaging is taken over the time. The characteristic correlation time for the ith neuron is then evaluated as $\tau_{i,C} = 1/T\int_T c_i^2(t)dt$ [30]. In the present case of limited and discrete sampling with N_0 data points for each neuron, the characteristic correlation time is given by

$$\tau_{i,C} = \frac{1}{N_0 \Delta t}\sum_{k=1}^{N} c_i^2(\tau_k)\Delta t, \tag{16}$$

where $\tau_k = k\Delta t$ with Δt being the sampling time, and $N_0\Delta t$ being the length of the time series.

Then the "order parameter" for given p is defined as

$$\tau(p) = [\langle \tau_{i,C}\rangle], \tag{17}$$

where $\langle\cdot\rangle$ denotes the average over all the neurons and $[\cdot]$ the average over 50 different network realizations with the same p. The more ordered a neuron bursting is, the longer is its characteristic correlation time and hence its contribution to the order parameter. Therefore, this quantity can be readily used to measure the degree of the spatiotemporal order in the present system [18]. At $D=0.05$ and $g=0.002$, the dependence of autocorrelation on the fraction of random shortcuts p is presented in Fig. 4 (line with circles). It has a clear maximum at $p=0.26$, where all neurons almost run periodically with the same phase.

The standard deviation σ is defined as

$$\sigma = [\{\sigma(t)\}]$$

with

$$\sigma(t) = \sqrt{\left[\frac{1}{N}\sum_{i=1}^{N} V_i(t)^2 - \left(\frac{1}{N}\sum_{i=1}^{N} V_i(t)\right)^2\right]} \Big/ \sqrt{(N-1)}, \tag{18}$$

where $\{\cdot\}$ denotes the average over time and $[\cdot]$ has the same meaning as above. Figure 5 depicts the dependence of σ on p of the network topology (line with circles). One can see that σ decreases monotonously when p is increased, approaching zero as $p \to 1$, which implies that the synchronization of the coupled MHH neurons is enhanced as p increases, and complete connections, i.e., $p \to 1$, will lead to the complete synchronization of the system.

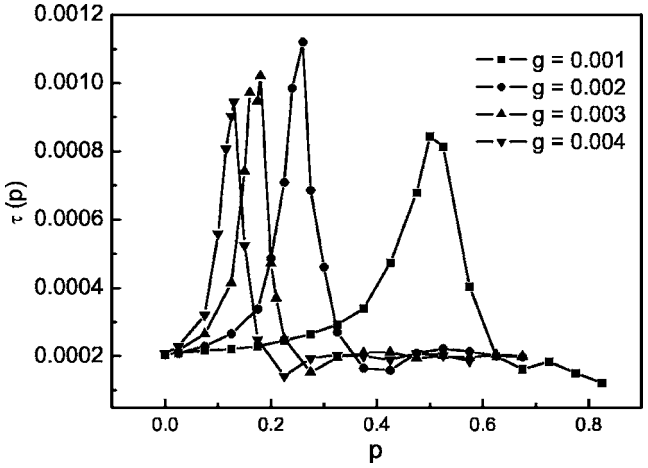

FIG. 4. Characteristic correlation time τ vs p at $D=0.05$ for $g=0.001, 0.002, 0.003, 0.004$, respectively. There is a peak in each curve of τ, indicating the occurrence of most ordered temporal behavior. The value of p for the peak shifts to a smaller value with increasing coupling constant g.

We have also studied the influence of coupling strength on the phenomenon. We carried out the calculations for other three coupling constants $g=0.001, 0.003, 0.004$ with noise level $D=0.05$. Similar evolutions of spatiotemporal patterns are found but with a somewhat difference in the degree of temporal regulation and spatial synchronization when the most ordered spatiotemporal patterns appear (not shown). We find that the most ordered spatiotemporal pattern at $g=0.002$ is more pronounced than others, which means in this case of coupling that the addition of random shortcuts may be more effective for the system to achieve a periodic spatiotemporal state than in other coupling values. The varia-

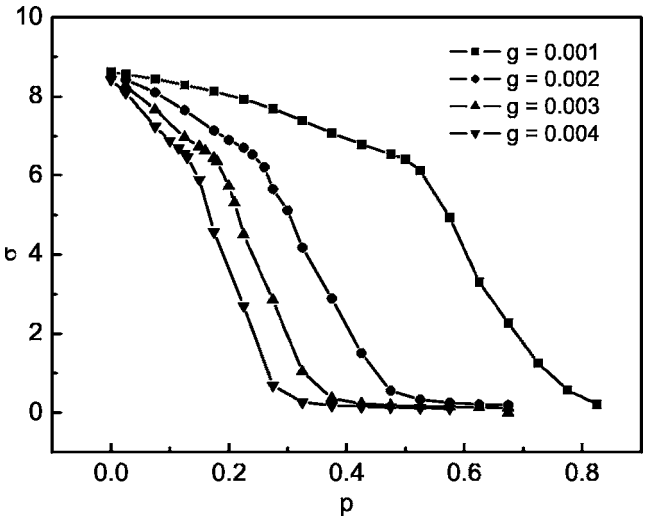

FIG. 5. Standard deviation σ vs p at $D=0.05$ for $g=0.001, 0.002, 0.003, 0.004$. The value of σ decreases with the increase of p, showing that the system becomes more and more synchronized. And σ decreases more rapidly with p for a stronger coupling constant; represent that same number of random connections makes the system reach synchronization more easily at a stronger coupling.

tions of the characteristic correlation time and the standard deviation with p at the other three coupling constants $g=0.001, 0.003, 0.004$ are also plotted in Figs. 4 and 5, respectively. One sees from Fig. 4 that the optimal randomness p shifts to a smaller number with the increase of g, which indicates that the larger g number, the smaller the number of randomly added shortcuts is needed for the system to achieve a periodic spatiotemporal pattern. In addition, the maximal value of τ for $g=0.002$ is larger than those for the other values of g, which indicates that a more pronounced spatiotemporal pattern appears in this case. Figure 5 shows that the larger the g number, the more rapidly the standard deviation decreases with increasing p, which represents that the system reaches spatial synchronization more effectively for a higher g.

To check the effect of larger or smaller noise levels, we have also calculated the characteristic correlation time and standard deviation for the other three typical noise levels $D=0.1, 0.005, 0.0005$ at $g=0.002$. We find that for different values of D the spatiotemporal patterns change slightly and the evolution of the characteristic correlation time and of the standard deviation with changing p is almost kept unchanged (figures not shown), which means that the variation of the appropriate noise level exerts a slight influence on the bursting activity and the spatiotemporal patterns are robust to it. This result for the model with temperature $T=8.2\ ^{\circ}\mathrm{C}$ qualitatively agrees with the conclusion for low temperature that the noise simply produces more realistic looking simulation and is necessary to account for subthreshold oscillations with skippings when high-temperature ranges are considered [28]. As a matter of fact, the addition of noise to the model in this work is for the purpose of checking the robustness of the result and for making the model more realistic.

In our previous work, it was also found that random shortcuts can tame spatiotemporal chaos in an array of coupled pendulum networks [18], and a sufficient number of random shortcuts will synchronize the behavior of the HH neurons [31]. In this work, we find similar result in the coupled MHH neuron networks. However, this work differs from the work in [31]: In that work, we used the HH model which is independent of temperature, and each HH neuron can merely fire regular spikes and cannot exhibit chaotic firings. While in this work, the coupled thermoreceptor neurons are taken as our model; more importantly, each neuron fires bursts which are more complex than spikes in dynamical behavior; and most importantly, each neuron initially stays in a chaotic firing state, and the ordering of it is just our main object in the present work.

By the results obtained above, it seems that ordering spatiotemporal chaos and enhanced synchronization and coherence by the optimal random network topology might be common phenomena. Our present findings, however, show that the spatiotemporal chaos in the neurons in the brain can also be tamed by an optimal number of random links between the neurons, which illustrates the importance of random links to the transfer of information in brain. The possible mechanism of this phenomenon, as stated in our previous work [18], may be understood as follows: At the early stage, a few random shortcuts between neurons can create local coherent structures, which bring the neuron chain into a periodic motion, and adding shortcuts could increase the number of coherent structures, which results in the growth of the characteristic correlation time. Meanwhile, the shortcuts can certainly enhance the synchronization of the coherent structures, and when the random shortcuts are optimal, the coherent structure could reach both a nearly synchronized and most periodic motion. However, if more shortcuts are added, the coupling between the neurons is so strong that the whole system behaves like a single chaotic neuron before coherent structures are formed, which results in worse periodicity in time and better synchronization in space.

How the present work could find its applications in real neural systems is an interesting question. On the one hand, synchronized neural activities in the central nervous system have been observed, and they may play an important role in revealing communication pathways in neural systems [32,33]. In addition, real neurons display rather rich dynamical behaviors such as chaos [34], and spatiotemporal chaos is viewed as a "waiting" state for the cortex, and hence the neurons in this waiting state exhibit the highly irregular spiking activities [35]. On the other hand, real neural systems are more feasible to be described as a complex network rather than a regular one. Therefore, the present findings provide an insight into understanding the properties of collective motions in coupled chaotic neurons and the exchange of information between different neuron states.

IV. CONCLUSION

We have studied the spatial synchronization and coherence of the chaotic MHH thermosensitive neurons on the complex networks. We find that the synchronization and coherence which are absent in the regular network can be greatly enhanced by random shortcuts between the neurons. In particular, we show that there exists an optimal randomness p at which the characteristic correlation time τ of the system is maximal, which corresponds to a most ordered spatiotemporal state that is the most periodic in time and nearly synchronized in space. Our findings provide an example that an optimal number of random shortcuts can effectively tame spatiotemporal chaos in the coupled MHH neurons. We also show that this phenomenon is robust to the change of the coupling strength and the noise level. And it is easier to tame the chaos under a stronger coupling, but the variation of an appropriate noise level hardly influences the spatiotemporal patterns. We expect that these results can find their applications in real neural systems.

ACKNOWLEDGMENTS

This work was supported by the National Science Foundation of China (Grant Nos. 20203017 and 20433050), the Foundation for the Author of National Excellent Doctoral Dissertation of P.R China (FANEDD), and the Doctoral Science Research Foundation of Yantai Normal University (Grant No. 23140301).

[1] S. N. Dorogovtsev and J. F. F. Mendes, Adv. Phys. **51**, 1079 (2002).
[2] R. Albert and A.-L. Barabasi, Rev. Mod. Phys. **74**, 47 (2002).
[3] S. H. Strogatz, Nature (London) **410**, 268 (2001).
[4] D. J. Watts and S. H. Strogatz, Nature (London) **393**, 440 (1998).
[5] A.-L. Barabasi and R. Albert, Science **286**, 509 (1999).
[6] M. E. J. Newman, Proc. Natl. Acad. Sci. U.S.A. **98**, 404 (2001).
[7] H. Jeong *et al.*, Nature (London) **411**, 41 (2001).
[8] J. Camacho *et al.*, Phys. Rev. Lett. **88**, 228102 (2002).
[9] S. Lawrence and C. L. Giles, Science **280**, 98 (1998).
[10] S. Lawrence and C. L. Giles, Nature (London) **400**, 107 (1999).
[11] R. Albert *et al.*, Nature (London) **401**, 130 (1999).
[12] R. Pastor-Satorras and A. Vespignani, Phys. Rev. Lett. **86**, 3200 (2001).
[13] R. Pastor-Satorras, Phys. Rev. E **65**, 035108 (2002).
[14] Z. Gao *et al.*, Phys. Rev. E **65**, 016209 (2002).
[15] M. Barahona and L. M. Pecora, Phys. Rev. Lett. **89**, 054101 (2002).
[16] H. Hong *et al.*, Phys. Rev. E **65**, 026139 (2002).
[17] D. He *et al.*, Phys. Rev. E **65**, 055204 (2002).
[18] F. Qi *et al.*, Phys. Rev. Lett. **91**, 064102 (2003).
[19] Z. H. Hou and H. W. Xin, Phys. Rev. E **68**, 055103 (2003).
[20] W. Gerstner and W. M. Kistler, in *Spiking Neuron Models* (Cambridge University Press, Cambridge, 2002).
[21] M. A. L. Nicolelis *et al.*, Science **268**, 1353 (1995).
[22] W. Wang *et al.*, Phys. Rev. E **56**, 3728 (1997).
[23] M. Steriade *et al.*, J. Neurophysiol. **79**, 483 (1998).
[24] H. A. Braun *et al.*, Int. J. Bifurcation Chaos Appl. Sci. Eng. **8**, 881 (1998).
[25] H. A. Braun *et al.*, Nature (London) **367**, 270 (1994).
[26] H. A. Braun *et al.*, J. Comp. Neurol. **4**, 335 (1997).
[27] S. Bahar, Fluct. Noise Lett. **4**, L87 (2004).
[28] U. Feudel *et al.*, Chaos **10**, 231 (2000).
[29] W. Braun *et al.*, Phys. Rev. E **62**, 6352 (2000).
[30] A. S. Pikovsky and J. Kurths, Phys. Rev. Lett. **78**, 775 (1997).
[31] Y. B. Gong *et al.*, ChemPhysChem **6**, 1042 (2005).
[32] C. M. Gray *et al.*, Nature (London) **338**, 334 (1989).
[33] R. Eckhorn *et al.*, Biol. Cybern. **60**, 121 (1988).
[34] J. Guckenheimer and R. A. Oliva, SIAM J. Appl. Dyn. Syst. **1**, 105 (2002).
[35] M. I. Rabinovich and H. D. I. Abarbanel, Neuroscience (Oxford) **87**, 5 (1998).